

RECEIVED: March 24, 2017

REVISED: August 1, 2017

ACCEPTED: August 6, 2017

PUBLISHED: August 25, 2017

# $B_s \rightarrow K \ell \nu_\ell$ and $B_{(s)} \rightarrow \pi(K) \ell^+ \ell^-$ decays at large recoil and CKM matrix elements

Alexander Khodjamirian<sup>a</sup> and Aleksey V. Rusov<sup>a,b</sup>

<sup>a</sup>*Theoretische Physik 1, Naturwissenschaftlich-Technische Fakultät, Universität Siegen, D-57068 Siegen, Germany*

<sup>b</sup>*Department of Theoretical Physics, P.G. Demidov Yaroslavl State University, 150000, Yaroslavl, Russia*

*E-mail:* [khodjamirian@physik.uni-siegen.de](mailto:khodjamirian@physik.uni-siegen.de), [rusov@physik.uni-siegen.de](mailto:rusov@physik.uni-siegen.de)

**ABSTRACT:** We provide hadronic input for the  $B$ -meson semileptonic transitions to a light pseudoscalar meson at large recoil. The  $B_s \rightarrow K$  form factor calculated from QCD light-cone sum rule is updated, to be used for a  $|V_{ub}|$  determination from the  $B_s \rightarrow K \ell \nu$  width. Furthermore, we calculate the hadronic input for the binned observables of  $B \rightarrow \pi \ell^+ \ell^-$  and  $B \rightarrow K \ell^+ \ell^-$ . In addition to the form factors, the nonlocal hadronic matrix elements are obtained, combining QCD factorization and light-cone sum rules with hadronic dispersion relations. We emphasize that, due to nonlocal effects, the ratio of branching fractions of these decays is not sufficient for an accurate extraction of the  $|V_{td}/V_{ts}|$  ratio. Instead, we suggest to determine the Wolfenstein parameters  $A, \rho, \eta$  of the CKM matrix, combining the branching fractions of  $B \rightarrow K \ell^+ \ell^-$  and  $B \rightarrow \pi \ell^+ \ell^-$  with the direct  $CP$ -asymmetry in the latter decay. We also obtain the hadronic matrix elements for a yet unexplored channel  $B_s \rightarrow K \ell^+ \ell^-$ .

**KEYWORDS:** Heavy Quark Physics, CP violation

ARXIV EPRINT: [1703.04765](https://arxiv.org/abs/1703.04765)

---

**Contents**

<b>1</b>	<b>Introduction</b>	<b>1</b>
<b>2</b>	<b>Observables in semileptonic <math>B_{(s)}</math> decays and CKM parameters</b>	<b>2</b>
<b>3</b>	<b>Numerical results</b>	<b>7</b>
<b>4</b>	<b>Discussion</b>	<b>13</b>
<b>A</b>	<b>LCSR calculation of the <math>B \rightarrow P</math> form factors</b>	<b>14</b>
<b>B</b>	<b>Nonlocal contributions to <math>B \rightarrow P\ell^+\ell^-</math></b>	<b>15</b>

---

**1 Introduction**

Determination of CKM matrix elements from the semileptonic decays of  $B$  meson remains a topical problem. Most importantly, one has to clarify the origin of the tension between the  $|V_{ub}|$  values extracted from the exclusive  $B \rightarrow \pi\ell\nu_\ell$  and inclusive  $B \rightarrow X_u\ell\nu_\ell$  decays (see e.g., the review [1]). The  $B \rightarrow \pi$  vector form factor  $f_{B\pi}^+(q^2)$  is the only theory input sufficient for the  $|V_{ub}|$  determination from  $B \rightarrow \pi\ell\nu_\ell$ . This hadronic matrix element is calculated in the lattice QCD at small recoil of the pion (at large  $q^2$ ) or from QCD light-cone sum rules (LCSRs) at large recoil of the pion (at small and intermediate  $q^2$ ).

Apart from increasing the accuracy of the form factor calculation, it is important to extend the set of “standard” exclusive processes used for  $|V_{ub}|$  determination. The  $B_s \rightarrow K^*(\rightarrow K\pi)\ell\nu_\ell$  decay, as one possibility, was discussed in [2]. A simpler process is the  $B_s \rightarrow K\ell\nu_\ell$  decay, where the data are anticipated from LHCb collaboration. Our first goal in this paper is to provide this decay mode with a hadronic input, updating the calculation of the  $B_s \rightarrow K$  form factors from LCSRs. This method [3–5] is based on the operator-product expansion (OPE) of a correlation function expressed in terms of light-meson distribution amplitudes (DAs) with growing twist. The violation of the  $SU(3)_{fl}$  symmetry in  $B_s \rightarrow K$  with respect to  $B \rightarrow \pi$  transition emerges in LCSRs due to the  $s$ -quark mass effects in the correlation function, including the asymmetry between the  $s$ - and  $\{u, d\}$ -partons in the kaon DAs. Earlier LCSR results on the  $B_s \rightarrow K$  form factors can be found in [6], where the NLO corrections to the correlation function computed in [7] were taken into account. In this paper we update the LCSRs for  $f_{B_s K}^+(q^2)$  and also for the tensor form factor  $f_{B_s K}^T(q^2)$ . In particular, we correct certain terms in the subleading twist-3,4 contributions to LCSRs for both vector and tensor form factors. In parallel, we recalculate the  $B \rightarrow K$  and  $B \rightarrow \pi$  form factors using a common set of input parameters, e.g., the updated [8] 2-point QCD sum rule for the decay constants  $f_B$  and  $f_{B_s}$ . Importantly, the twist-5,6 corrections to the LCSRs estimated by one of us [9] are negligibly small, ensuring the reliability of the adopted twist  $\leq 4$  approximation.

The calculated form factors are then used to address the second goal of this paper: determination of CKM parameters from the flavour-changing neutral current (FCNC) decays  $B \rightarrow K\ell^+\ell^-$ ,  $B \rightarrow \pi\ell^+\ell^-$  and  $B_s \rightarrow K\ell^+\ell^-$ . Recently,  $|V_{td}|$ ,  $|V_{ts}|$  and their ratio were determined by LHCb collaboration [10] from the measured  $B \rightarrow \pi\ell^+\ell^-$  and  $B \rightarrow K\ell^+\ell^-$  partial widths. We suggest to make the extraction of CKM parameters from these decays more accurate and comprehensive. As well known, in addition to the semileptonic form factors, the hadronic input in FCNC decays includes also nonlocal hadronic matrix elements emerging due to the electromagnetic lepton-pair emission combined with the weak transitions. These hadronic matrix elements in the  $B \rightarrow \pi\ell^+\ell^-$  decay amplitude are multiplied by the CKM parameters other than  $V_{td}$ , making the determination of the latter not straightforward. We take into account the nonlocal hadronic effects in  $B \rightarrow K\ell^+\ell^-$  and  $B \rightarrow \pi\ell^+\ell^-$ , employing the methods used in [12, 13] and originally suggested in [11]. The nonlocal hadronic matrix elements are calculated at spacelike  $q^2$ , using OPE, QCD factorization [14] and LCSRs, and are then matched to their values at timelike  $q^2$  via hadronic dispersion relations. The results of this calculation are reliable at large hadronic recoil, below the charmonium region, that is, at  $q^2 < m_{J/\psi}^2$ . Here we also extend the calculation of nonlocal effects to the previously unexplored channel  $B_s \rightarrow K\ell^+\ell^-$ .

The binned widths and direct  $CP$ -asymmetries of FCNC semileptonic decays are then expressed in a form combining the CKM parameters with the quantities determined by the calculated hadronic input. Here we find it more convenient to switch to the Wolfenstein parametrization of the CKM matrix. In this form, three observables: the width of  $B \rightarrow K\ell^+\ell^-$ , the ratio of  $B \rightarrow \pi\ell^+\ell^-$  and  $B \rightarrow K\ell^+\ell^-$  widths and the direct  $CP$ -asymmetry in  $B \rightarrow \pi\ell^+\ell^-$ , are sufficient to extract the three Wolfenstein parameters  $A$ ,  $\eta$  and  $\rho$  from experimental data, provided the parameter  $\lambda$  is known quite precisely. Two additional observables for the same determination are given by the yet unobserved  $B_s \rightarrow K\ell^+\ell^-$  decay. The current data on the  $B \rightarrow K\ell^+\ell^-$  and  $B \rightarrow \pi\ell^+\ell^-$  decays are not yet precise enough to yield the CKM parameters with an accuracy comparable to the other determinations. Hence, here we limit ourselves with the Wolfenstein parameters taken from the global CKM fit and predict the binned observables of all three FCNC decays in the optimal interval  $1.0 \text{ GeV}^2 < q^2 < 6.0 \text{ GeV}^2$  of the large recoil region.

In what follows, in section 2 we specify and discuss the hadronic input and observables in the exclusive semileptonic  $B_{(s)}$  decays. In section 3 we present the numerical results and section 4 is devoted to the final discussion. In the appendices, we briefly recapitulate the calculation A of the form factors from LCSRs and B of the nonlocal hadronic matrix elements.

## 2 Observables in semileptonic $B_{(s)}$ decays and CKM parameters

The form factors of semileptonic transitions of  $B$ -meson to a light pseudoscalar meson  $P = \pi, K$  are defined in a standard way:

$$\langle P(p) | \bar{q} \gamma^\mu b | B(p+q) \rangle = f_{BP}^+(q^2) \left[ 2p^\mu + \left( 1 - \frac{m_B^2 - m_P^2}{q^2} \right) q^\mu \right] + f_{BP}^0(q^2) \frac{m_B^2 - m_P^2}{q^2} q^\mu, \quad (2.1)$$

$$\langle P(p) | \bar{q} \sigma^{\mu\nu} q_\nu b | B(p+q) \rangle = \frac{i f_{BP}^T(q^2)}{m_B + m_P} \left[ 2q^2 p^\mu + \left( q^2 - (m_B^2 - m_P^2) \right) q^\mu \right], \quad (2.2)$$

where  $p^\mu$  and  $q^\mu$  are the four-momenta of the  $P$ -meson and lepton pair, respectively, and the vector and scalar form factors coincide at  $q^2 = 0$ , that is,  $f_{BP}^+(0) = f_{BP}^0(0)$ .

We start from the weak semileptonic decay  $\bar{B}_s \rightarrow K^+ \ell \bar{\nu}_\ell$ , where the hadronic input for  $\ell = e, \mu$  in the  $m_\ell = 0$  approximation is given by the vector form factor  $f_{B_s K}^+$ . We use the following quantity related to the differential width integrated over an interval  $0 \leq q^2 \leq q_0^2$ :

$$\Delta\zeta_{B_s K}[0, q_0^2] \equiv \frac{G_F^2}{24\pi^3} \int_0^{q_0^2} dq^2 p_{B_s K}^3 |f_{B_s K}^+(q^2)|^2 = \frac{1}{|V_{ub}|^2 \tau_{B_s}} \int_0^{q_0^2} dq^2 \frac{dB(\bar{B}_s \rightarrow K^+ \ell \bar{\nu}_\ell)}{dq^2}, \quad (2.3)$$

where the  $q^2$ -dependent kinematical factor  $p_{BP} = [(m_B^2 + m_P^2 - q^2)^2 / (4m_B^2) - m_P^2]^{1/2}$  is the 3-momentum of  $P$  meson in the rest frame of  $B$  meson. Our choice for the integration interval is  $q_0^2 = 12.0 \text{ GeV}^2$ , covering the region where the LCSRs used for the calculation of the form factors (see appendix A) are valid. The same interval was adopted for the analogous quantity  $\Delta\zeta_{B\pi}[0, q_0^2]$  for  $B \rightarrow \pi \ell \nu_\ell$  calculated in [15, 16]. The numerical estimate of  $\Delta\zeta_{B_s K}[0, q_0^2]$  presented in the next section can be directly used for  $|V_{ub}|$  determination, provided the integrated branching fraction on the r.h.s. of eq. (2.3) is measured.

Turning to semileptonic decays generated by the  $b \rightarrow s(d)\ell^+\ell^-$  transitions ( $\ell = e, \mu$ ), we use a generic notation  $\bar{B} \rightarrow P\ell^+\ell^-$  for the three channels:  $B^- \rightarrow K^-\ell^+\ell^-$ ,  $B^- \rightarrow \pi^-\ell^+\ell^-$  and  $\bar{B}_s \rightarrow K^0\ell^+\ell^-$ ,<sup>1</sup> denoting the  $CP$  conjugated channels by  $B \rightarrow \bar{P}\ell^+\ell^-$ . The decay amplitude can be represented in the following form:

$$A(\bar{B} \rightarrow P\ell^+\ell^-) = \frac{G_F \alpha_{\text{em}}}{\sqrt{2} \pi} \left\{ \left[ \lambda_t^{(q)} f_{BP}^+(q^2) c_{BP}(q^2) + \lambda_u^{(q)} d_{BP}(q^2) \right] (\bar{\ell} \gamma^\mu \ell) p_\mu + \lambda_t^{(q)} C_{10} f_{BP}^+(q^2) (\bar{\ell} \gamma^\mu \gamma_5 \ell) p_\mu \right\}, \quad (2.4)$$

where  $\lambda_p^{(q)} = V_{pb} V_{pq}^*$  ( $p = u, c, t$ ;  $q = d, s$ ),  $m_\ell = 0$ , and we use unitarity of the CKM matrix, fixing hereafter  $\lambda_c^{(q)} = -(\lambda_t^{(q)} + \lambda_u^{(q)})$ . In eq. (2.4) we introduce a compact notation:

$$c_{BP}(q^2) = C_9 + \frac{2(m_b + m_q)}{m_B + m_P} C_7^{\text{eff}} \frac{f_{BP}^T(q^2)}{f_{BP}^+(q^2)} + 16\pi^2 \frac{\mathcal{H}_{BP}^{(c)}(q^2)}{f_{BP}^+(q^2)}, \quad (2.5)$$

where  $m_q$  is the mass of  $d$  or  $s$ -quark and

$$d_{BP}(q^2) = 16\pi^2 \left( \mathcal{H}_{BP}^{(c)}(q^2) - \mathcal{H}_{BP}^{(u)}(q^2) \right). \quad (2.6)$$

In addition, we introduce the phase difference of the hadronic amplitudes defined above:

$$\delta_{BP}(q^2) = \text{Arg}(d_{BP}(q^2)) - \text{Arg}(c_{BP}(q^2)). \quad (2.7)$$

In eq. (2.4) the dominant contributions of the operators  $O_{9,10}$  and  $O_{7\gamma}$  of the effective Hamiltonian (see appendix B) are expressed in terms of the vector and tensor  $B \rightarrow P$

---

<sup>1</sup>For simplicity we consider a transition into the fixed flavour state  $K^0$  which is easy to convert to  $K_s$  if needed.

form factors,  $f_{BP}^+(q^2)$  and  $f_{BP}^T(q^2)$ , respectively, defined in eqs. (2.1) and (2.2). The amplitudes  $\mathcal{H}_{BP}^{(c,u)}(q^2)$  parametrize the nonlocal contributions to  $B \rightarrow P\ell^+\ell^-$ , generated by the current-current, quark-penguin and chromomagnetic operators in the effective Hamiltonian, combined with an electromagnetically produced lepton pair. The definition of nonlocal amplitudes is given in appendix B, where also the method of their calculation is briefly explained. In refs. [11, 12], this part of hadronic input was cast in the form of an effective (process- and  $q^2$ -dependent) addition  $\Delta C_9^{BP}(q^2)$  to the Wilson coefficient  $C_9$ . Here, as in ref. [13], we find it more convenient to separate the parts proportional to  $\lambda_u^{(q)}$  and  $\lambda_c^{(q)} = -(\lambda_t^{(q)} + \lambda_u^{(q)})$ .

Squaring the amplitude (2.4) and integrating over the phase space, one obtains for the  $q^2$ -binned branching fraction, defined as:

$$\mathcal{B}(\bar{B} \rightarrow P\ell^+\ell^-[q_1^2, q_2^2]) \equiv \frac{1}{q_2^2 - q_1^2} \int_{q_1^2}^{q_2^2} dq^2 \frac{dB(\bar{B} \rightarrow P\ell^+\ell^-)}{dq^2}, \quad (2.8)$$

the following expression:

$$\begin{aligned} \mathcal{B}(\bar{B} \rightarrow P\ell^+\ell^-[q_1^2, q_2^2]) = \frac{G_F^2 \alpha_{\text{em}}^2 |\lambda_t^{(q)}|^2}{192\pi^5} & \left\{ \mathcal{F}_{BP}[q_1^2, q_2^2] + \kappa_q^2 \mathcal{D}_{BP}[q_1^2, q_2^2] \right. \\ & \left. + 2\kappa_q \left( \cos \xi_q \mathcal{C}_{BP}[q_1^2, q_2^2] - \sin \xi_q \mathcal{S}_{BP}[q_1^2, q_2^2] \right) \right\} \tau_B, \end{aligned} \quad (2.9)$$

where the ratio of CKM matrix elements is parametrized in terms of its module and phase:

$$\frac{\lambda_u^{(q)}}{\lambda_t^{(q)}} = \frac{V_{ub}V_{uq}^*}{V_{tb}V_{tq}^*} \equiv \kappa_q e^{i\xi_q}, \quad (q = d, s), \quad (2.10)$$

and we use the following notation for the phase-space weighted and integrated parts of the decay amplitude squared:

$$\mathcal{F}_{BP}[q_1^2, q_2^2] = \frac{1}{q_2^2 - q_1^2} \int_{q_1^2}^{q_2^2} dq^2 p_{BP}^3 |f_{BP}^+(q^2)|^2 \left( |c_{BP}(q^2)|^2 + |C_{10}|^2 \right), \quad (2.11)$$

$$\mathcal{D}_{BP}[q_1^2, q_2^2] = \frac{1}{q_2^2 - q_1^2} \int_{q_1^2}^{q_2^2} dq^2 p_{BP}^3 |d_{BP}(q^2)|^2, \quad (2.12)$$

$$\mathcal{C}_{BP}[q_1^2, q_2^2] = \frac{1}{q_2^2 - q_1^2} \int_{q_1^2}^{q_2^2} dq^2 p_{BP}^3 |f_{BP}^+(q^2)c_{BP}(q^2)d_{BP}(q^2)| \cos \delta_{BP}(q^2), \quad (2.13)$$

$$\mathcal{S}_{BP}[q_1^2, q_2^2] = \frac{1}{q_2^2 - q_1^2} \int_{q_1^2}^{q_2^2} dq^2 p_{BP}^3 |f_{BP}^+(q^2)c_{BP}(q^2)d_{BP}(q^2)| \sin \delta_{BP}(q^2). \quad (2.14)$$

The binned branching fraction for the  $CP$ -conjugated mode  $B \rightarrow \bar{P}\ell^+\ell^-$  is obtained from eq. (2.9) by changing the sign at the term proportional to  $\sin \xi_q$ .

Furthermore, we consider two binned observables: the  $CP$ -averaged branching fraction:

$$\begin{aligned} \mathcal{B}_{BP}[q_1^2, q_2^2] &\equiv \frac{1}{2} (\mathcal{B}(\bar{B} \rightarrow P\ell^+\ell^- [q_1^2, q_2^2]) + \mathcal{B}(B \rightarrow \bar{P}\ell^+\ell^- [q_1^2, q_2^2])) \\ &= \frac{G_F^2 \alpha_{\text{em}}^2 |\lambda_t^{(q)}|^2}{192\pi^5} \left\{ \mathcal{F}_{BP}[q_1^2, q_2^2] + \kappa_q^2 \mathcal{D}_{BP}[q_1^2, q_2^2] + 2\kappa_q \cos \xi_q \mathcal{C}_{BP}[q_1^2, q_2^2] \right\} \tau_B, \end{aligned} \quad (2.15)$$

and the corresponding direct  $CP$ -asymmetry:

$$\begin{aligned} \mathcal{A}_{BP}[q_1^2, q_2^2] &= \frac{\mathcal{B}(\bar{B} \rightarrow P\ell^+\ell^- [q_1^2, q_2^2]) - \mathcal{B}(B \rightarrow \bar{P}\ell^+\ell^- [q_1^2, q_2^2])}{\mathcal{B}(\bar{B} \rightarrow P\ell^+\ell^- [q_1^2, q_2^2]) + \mathcal{B}(B \rightarrow \bar{P}\ell^+\ell^- [q_1^2, q_2^2])} \\ &= \frac{-2\kappa_q \sin \xi_q \mathcal{S}_{BP}[q_1^2, q_2^2]}{\mathcal{F}_{BP}[q_1^2, q_2^2] + \kappa_q^2 \mathcal{D}_{BP}[q_1^2, q_2^2] + 2\kappa_q \cos \xi_q \mathcal{C}_{BP}[q_1^2, q_2^2]}. \end{aligned} \quad (2.16)$$

In eqs. (2.15) and (2.16) the CKM-dependent coefficients are conveniently separated from the quantities  $\mathcal{F}_{BP}$ ,  $\mathcal{D}_{BP}$ ,  $\mathcal{C}_{BP}$ ,  $\mathcal{S}_{BP}$ , which contain the calculable hadronic matrix elements, Wilson coefficients and kinematical factors. In the next section we present numerical results for these quantities for a definite  $q^2$ -bin in the large-recoil region.

Turning to the observables for the specific decay channels, we neglect  $\lambda_u^{(s)}$ , hence, put  $\kappa_s = 0$  and obtain for  $B \rightarrow K\ell^+\ell^-$ :

$$\mathcal{B}_{BK}[q_1^2, q_2^2] = \frac{G_F^2 \alpha_{\text{em}}^2 |\lambda_t^{(s)}|^2}{192\pi^5} \mathcal{F}_{BK}[q_1^2, q_2^2] \tau_B, \quad (2.17)$$

with vanishing  $CP$  asymmetry. For  $B^- \rightarrow \pi^-\ell^+\ell^-$  and its  $CP$ -conjugated process both observables,

$$\mathcal{B}_{B\pi}[q_1^2, q_2^2] = \frac{G_F^2 \alpha_{\text{em}}^2 |\lambda_t^{(d)}|^2}{192\pi^5} \left\{ \mathcal{F}_{B\pi}[q_1^2, q_2^2] + \kappa_d^2 \mathcal{D}_{B\pi}[q_1^2, q_2^2] + 2\kappa_d \cos \xi_d \mathcal{C}_{B\pi}[q_1^2, q_2^2] \right\} \tau_B, \quad (2.18)$$

and

$$\mathcal{A}_{B\pi}[q_1^2, q_2^2] = \frac{-2\kappa_d \sin \xi_d \mathcal{S}_{B\pi}[q_1^2, q_2^2]}{\mathcal{F}_{B\pi}[q_1^2, q_2^2] + \kappa_d^2 \mathcal{D}_{B\pi}[q_1^2, q_2^2] + 2\kappa_d \cos \xi_d \mathcal{C}_{B\pi}[q_1^2, q_2^2]}, \quad (2.19)$$

are relevant. The corresponding observables  $\mathcal{B}_{B_s K}[q_1^2, q_2^2]$  and  $\mathcal{A}_{B_s K}[q_1^2, q_2^2]$  for  $\bar{B}_s \rightarrow K^0\ell^+\ell^-$  and its  $CP$ -conjugated mode are given by the expressions similar to eqs. (2.18), (2.19), with  $B\pi$  replaced by  $B_s K$ . Here we do not consider the decays  $\bar{B}^0 \rightarrow \bar{K}^0\ell^+\ell^-$  and  $\bar{B}^0 \rightarrow \pi^0\ell^+\ell^-$ , which are the isospin counterparts of, respectively,  $B^- \rightarrow K^-\ell^+\ell^-$  and  $B^- \rightarrow \pi^-\ell^+\ell^-$  and can be treated in a similar way (see [12, 13]). We also postpone to a future study the time-dependent  $CP$ -asymmetry in the  $\bar{B}_s \rightarrow K^0\ell^+\ell^-$  decay.

Dividing eq. (2.18) by eq. (2.17), we notice that an accurate extraction of the ratio  $|V_{td}/V_{ts}|$  from the ratio of branching fractions  $\mathcal{B}_{B\pi}[q_1^2, q_2^2]/\mathcal{B}_{BK}[q_1^2, q_2^2]$  can only be achieved

if the contributions of process-dependent nonlocal effects are taken into account for both decay modes. Moreover, this ratio depends also on the other CKM parameters, most importantly, on the  $V_{ub}$  value.<sup>2</sup>

Here we suggest a different, more systematic way to extract the parameters of CKM matrix from the observables (2.17)–(2.19). First of all, we find it more convenient to switch to the four standard Wolfenstein parameters  $\lambda$ ,  $A$ ,  $\rho$  and  $\eta$  defined as in [17]. The relevant CKM factors can be represented as follows:

$$\lambda_t^{(s)} = -A\lambda^2, \tag{2.20}$$

$$\left| \frac{\lambda_t^{(d)}}{\lambda_t^{(s)}} \right| = \left| \frac{V_{td}}{V_{ts}} \right| = \lambda \sqrt{(1-\rho)^2 + \eta^2}, \tag{2.21}$$

$$\frac{\lambda_u^{(d)}}{\lambda_t^{(d)}} = \frac{V_{ub}V_{ud}^*}{V_{tb}V_{td}^*} \equiv \kappa_d e^{i\xi_d} = \left(1 - \frac{\lambda^2}{2}\right) \frac{\rho(1-\rho) - \eta^2 - i\eta}{(1-\rho)^2 + \eta^2}, \tag{2.22}$$

so that

$$\kappa_d = \left(1 - \frac{\lambda^2}{2}\right) \frac{\sqrt{(\rho(1-\rho) - \eta^2)^2 + \eta^2}}{(1-\rho)^2 + \eta^2}, \tag{2.23}$$

$$\sin \xi_d = \frac{-\eta}{\sqrt{(\rho(1-\rho) - \eta^2)^2 + \eta^2}}, \quad \cos \xi_d = \frac{\rho(1-\rho) - \eta^2}{\sqrt{(\rho(1-\rho) - \eta^2)^2 + \eta^2}}, \tag{2.24}$$

where we neglect very small  $O(\lambda^4)$  corrections to these expressions.<sup>3</sup>

Hereafter, we suppose, that the parameter  $\lambda$ , precisely determined from the global CKM fit [17], is used as an input. Then, it is possible to extract all three remaining Wolfenstein parameters combining the three observables (2.17)–(2.19) for semileptonic FCNC decays. First, the parameter  $A$  is determined from the binned branching fraction of  $B \rightarrow K\ell^+\ell^-$ , as follows after substituting eq. (2.20) in eq. (2.17):

$$A = \frac{(192\pi^5)^{1/2}}{G_F\alpha_{em}\lambda^2} \left( \frac{1}{\mathcal{F}_{BK}[q_1^2, q_2^2]} \right)^{1/2} \left( \frac{\mathcal{B}_{BK}[q_1^2, q_2^2]}{\tau_B} \right)^{1/2}. \tag{2.25}$$

Then, combining the ratio of the  $B \rightarrow \pi\ell^+\ell^-$  and  $B \rightarrow K\ell^+\ell^-$  binned branching fractions with the  $CP$ -asymmetry of the pion mode, and employing eqs. (2.21), (2.23) and (2.24), we obtain for the parameter  $\eta$  the following relation:

$$\eta = \frac{1}{2\lambda^2(1-\lambda^2/2)} \left( \frac{\mathcal{F}_{BK}[q_1^2, q_2^2]}{\mathcal{S}_{B\pi}[q_1^2, q_2^2]} \right) \left( \mathcal{A}_{B\pi}[q_1^2, q_2^2] \frac{\mathcal{B}_{B\pi}[q_1^2, q_2^2]}{\mathcal{B}_{BK}[q_1^2, q_2^2]} \right). \tag{2.26}$$

<sup>2</sup>Note that in the analysis of  $B \rightarrow \pi\ell^+\ell^-$  and  $B \rightarrow K\ell^+\ell^-$  presented in [10] these effects are not explicitly specified.

<sup>3</sup>This is consistent with neglecting the  $O(\lambda_u^{(s)}) \sim O(\lambda^4)$  terms in the  $B \rightarrow K\ell^+\ell^-$  amplitude. These terms contain nonlocal effects generated by the  $u$ -quark loops and calculable within our approach. Hence, achieving the  $O(\lambda^4)$  precision is possible in future.

Parameter	Ref.
$G_F = 1.1664 \times 10^{-5} \text{ GeV}^2$ ; $\alpha_{em} = 1/129$ $\alpha_s(m_Z) = 0.1185 \pm 0.0006$ ; $\alpha_s(3 \text{ GeV}) = 0.252$ $\bar{m}_b(\bar{m}_b) = 4.18 \pm 0.03 \text{ GeV}$ ; $\bar{m}_c(\bar{m}_c) = 1.275 \pm 0.025 \text{ GeV}$ $\bar{m}_s(2 \text{ GeV}) = 95 \pm 10 \text{ MeV}$	[17]
$\mu = 3.0_{-0.5}^{+1.5} \text{ GeV}$	
$f_\pi = 130.4 \text{ MeV}$ ; $f_K = 159.8 \text{ MeV}$	[17]
$a_2^\pi(1 \text{ GeV}) = 0.17 \pm 0.08$ ; $a_4^\pi(1 \text{ GeV}) = 0.06 \pm 0.10$	[15]
$a_1^K(1 \text{ GeV}) = 0.10 \pm 0.04$ ; $a_2^K(1 \text{ GeV}) = 0.25 \pm 0.15$	[18, 19]
$\mu_\pi(2 \text{ GeV}) = 2.50 \pm 0.30 \text{ GeV}$ ; $\mu_K(2 \text{ GeV}) = 2.49 \pm 0.26 \text{ GeV}$	[18, 20]
$M^2 = 16 \pm 4 \text{ GeV}^2$ ( $M^2 = 17 \pm 4 \text{ GeV}^2$ ) [in $B(B_s)$ -channel]	[15]
$\lambda_B = 460 \pm 110 \text{ MeV}$	[30]
$M^2 = 1.0 \pm 0.5 \text{ GeV}^2$ ; $s_0^\pi = 0.7 \text{ GeV}^2$ ; $s_0^K = 1.05 \text{ GeV}^2$	[11]

**Table 1.** Input parameters used in the numerical analysis.

Finally, after  $\eta$  is determined, the parameter  $\rho$  can be extracted from the ratio of branching fractions (2.18) and (2.17) written explicitly in terms of  $\eta$  and  $\rho$ :

$$\begin{aligned}
 \frac{\mathcal{B}_{B\pi}[q_1^2, q_2^2]}{\mathcal{B}_{BK}[q_1^2, q_2^2]} &= \frac{\lambda^2}{\mathcal{F}_{BK}[q_1^2, q_2^2]} \left( \left[ (1 - \rho)^2 + \eta^2 \right] \mathcal{F}_{B\pi}[q_1^2, q_2^2] \right. \\
 &\quad + \frac{[\rho(1 - \rho) - \eta^2]^2 + \eta^2}{(1 - \rho)^2 + \eta^2} \left( 1 - \frac{\lambda^2}{2} \right)^2 \mathcal{D}_{B\pi}[q_1^2, q_2^2] \\
 &\quad \left. + 2[\rho(1 - \rho) - \eta^2] \left( 1 - \frac{\lambda^2}{2} \right) \mathcal{C}_{B\pi}[q_1^2, q_2^2] \right). \quad (2.27)
 \end{aligned}$$

Similar relations for the  $B_s \rightarrow K\ell^+\ell^-$  decay, obtained by replacing  $B\pi \rightarrow B_s K$  in eqs. (2.26) and (2.27), provide an additional source of these parameters.

### 3 Numerical results

The most important input parameters used in our numerical analysis are listed in table 1. In particular, the electroweak parameters, the strong coupling and the meson masses are taken from [17]. For the quark masses in  $\overline{MS}$  scheme, entering the correlation functions for QCD sum rules, we adopt, following, e.g., [8], the intervals covering the non-lattice determinations in [17]. We put  $m_{u,d} = 0$ , except in the combination  $\mu_{\pi(K)} = m_{\pi(K)}^2 / (m_u + m_{d(s)})$  entering the pion and kaon DAs. In LCSRs, parameters of the pion and kaon twist-2 DA's include the decay constants, and the Gegenbauer moments  $a_{2,4}^\pi$  and  $a_{1,2}^K$ . Normalization of the twist-3 DAs is determined by  $\mu_{\pi,K}$ , where the ChPT relations [20] between light-quark masses are used (see e.g., [18]). The remaining parameters of the



Transition	$f_{BP}^+(0)$	$b_{1(BP)}^+$	Correlation
$B_s \rightarrow K$	$0.336 \pm 0.023$	$-2.53 \pm 1.17$	0.79
$B \rightarrow K$	$0.395 \pm 0.033$	$-1.42 \pm 1.52$	0.72
$B \rightarrow \pi$	$0.301 \pm 0.023$	$-1.72 \pm 1.14$	0.74
Transition	$f_{BP}^T(0)$	$b_{1(BP)}^T$	Correlation
$B_s \rightarrow K$	$0.320 \pm 0.019$	$-1.08 \pm 1.53$	0.74
$B \rightarrow K$	$0.381 \pm 0.027$	$-0.87 \pm 1.72$	0.75
$B \rightarrow \pi$	$0.273 \pm 0.021$	$-1.54 \pm 1.42$	0.78

**Table 2.** The fitted parameters of the  $z$ -expansion (3.1) for the vector (upper panel) and tensor (lower panel)  $B \rightarrow P$  form factors at  $0 < q^2 < 12.0 \text{ GeV}^2$  calculated from LCSRs.

twist-3 and twist-4 DAs, not shown in table 1 for brevity, are taken from [21], they were also used in [11, 15, 18]. Furthermore, in LCSRs the renormalization scale  $\mu$  and the Borel parameters  $M$  for the sum rules with  $B$  ( $B_s$ ) interpolating current quoted in table 1 are chosen, largely following [15]. The effective quark-hadron duality threshold is determined calculating the  $B_{(s)}$ -meson mass from the differentiated LCSR. The decay constants  $f_B$  and  $f_{B_s}$  entering LCSRs are replaced by the two-point sum rules in NLO, their expressions and input parameters (in particular, the vacuum condensate densities) are the same as in [8]. The intervals obtained from these sum rules in NLO are  $f_B = (202_{-21}^{+35}) \text{ MeV}$ ,  $f_{B_s} = (222_{-24}^{+38}) \text{ MeV}$ . Note that the above uncertainties are effectively smaller in LCSRs (eq. (A.4) in appendix A) due to the correlations of common parameters.

Using the input described above, we obtain the updated prediction for the  $B_s \rightarrow K$  vector and tensor form factors in the region  $0 \leq q^2 \leq 12.0 \text{ GeV}^2$  where the OPE for LCSRs in the adopted approximation is reliable (see appendix A). In parallel, we also recalculate the  $B \rightarrow K$  and  $B \rightarrow \pi$  form factors. For convenience, we fit the LCSR predictions for the  $B \rightarrow P$  form factors in this region to the two-parameter BCL-version of  $z$ -expansion [22] in the form adopted in [18]:

$$f_{BP}^{+,T}(q^2) = \frac{f_{BP}^{+,T}(0)}{1 - q^2/m_{B_{(s)}}^2} \left\{ 1 + b_{1(BP)}^{+,T} \left[ z(q^2) - z(0) + \frac{1}{2} (z(q^2)^2 - z(0)^2) \right] \right\}, \quad (3.1)$$

where

$$z(q^2) = \frac{\sqrt{t_+ - q^2} - \sqrt{t_+ - t_0}}{\sqrt{t_+ - q^2} + \sqrt{t_+ - t_0}}, \quad (3.2)$$

$$t_{\pm} = (m_B \pm m_P)^2, \quad t_0 = (m_B + m_P) \cdot (\sqrt{m_B} - \sqrt{m_P})^2, \quad (3.3)$$

and the pole mass in eq. (3.1) for  $B_s \rightarrow K$ ,  $B \rightarrow \pi$  ( $B \rightarrow K$ ) form factors is equal to  $m_{B^*}$  ( $m_{B_s^*}$ ). The fitted parameters of the vector and tensor form factors and their correlations are presented in table 2. Note that, adopting a more complicated  $z$ -expansion with more slope parameters, only insignificantly changes the quality of the fit, and reveals strong

correlations between these parameters. In any case the actual form of parametrization does not play a role as soon as we stay within the  $q^2$ -region where the form factors are directly calculated from LCSRs. Our results for the form factors are also plotted in figure 1, where the error bands correspond to the uncertainties of the fitted parameters shown in table 2. For comparison, we also show in the same figures the extrapolations of the recent lattice QCD results obtained at large  $q^2$  (low hadronic recoil) and continued to the small  $q^2$  region using the  $z$ -series parametrization. For the vector  $B_s \rightarrow K$  form factor this extrapolation was obtained by HPQCD Collaboration [23]. The same form factor was also calculated by ALPHA Collaboration [24] at a single large- $q^2$  value. For the vector and tensor  $B \rightarrow K$  form factors we compare our results with the extrapolations obtained from Fermilab Lattice and MILC Collaboration results [25], to which the HPQCD Collaboration results [26] are very close (not shown here). Finally, the low- $q^2$  extrapolations of the lattice  $B \rightarrow \pi$  vector and tensor form factors are taken from [27] and [28], respectively.

The knowledge of the  $B_s \rightarrow K$  vector form factor at large recoil enables us to calculate the quantity defined in eq. (2.3). The result

$$\Delta\zeta_{B_s K} [0, 12 \text{ GeV}^2] = 7.03_{-0.69}^{+0.73} \text{ ps}^{-1} \tag{3.4}$$

can be directly used for  $|V_{ub}|$  determination, provided the differential width of  $B_s \rightarrow K\ell\nu_\ell$  integrated over the same bin is measured. For comparison we recalculate the same quantity for  $B \rightarrow \pi\ell\nu_\ell$ :

$$\Delta\zeta_{B\pi} [0, 12 \text{ GeV}^2] = 5.30_{-0.63}^{+0.67} \text{ ps}^{-1}, \tag{3.5}$$

which is, as it should be, very close to the interval predicted in [16]. The latter interval is somewhat narrower than (3.5), reflecting the statistical (Bayesian) treatment applied in [16] which generally produces less conservative errors. In the future, when sufficiently accurate data on  $B_s \rightarrow K\ell\nu_\ell$  become available, a global statistical treatment of all  $B \rightarrow P$  form factors is desirable.

Comparing our results in table 2 with the earlier LCSR calculation [6] of the  $B \rightarrow K$  and  $B_s \rightarrow K$  form factors, we emphasize that, albeit the numerical results look close to ours, there are differences in the subleading twist-3,4 terms. We follow ref. [18] where these terms have already been discussed and corrected. Also, as compared to [6], we use slightly different  $B_{(s)}$  decay constants and twist-3 normalization parameter  $\mu_K$ .

Furthermore, the interval for our updated result for the  $B \rightarrow K$  vector form factor in table 2 lies somewhat above the previous LCSR prediction [11],  $f_{BK}^+(0) = 0.34_{-0.02}^{+0.05}$ , mainly due to the smaller value of  $f_B$  from the two-point sum rule used here and due to the slightly smaller value of the effective threshold in LCSR used in [11]. On the other hand, in the LCSR for  $f_{BK}^T(q^2)$  some minor corrections, implemented here in the subleading twist-4 terms, largely compensate the shift caused by the  $B$ -decay constant, so that our result in table 2 is close to  $f_{BK}^T(0) = 0.39_{-0.03}^{+0.05}$  obtained in [11].

Turning finally to the LCSR result for the vector  $B \rightarrow \pi$  form factor, which was updated several times in past, let us mention that although we use the same analytical expressions as in ref. [7], the input parameters such as  $\mu_\pi$  (determined by the light quark masses) and Gegenbauer moments  $a_2^\pi, a_4^\pi$  became more accurate, leading to a narrower

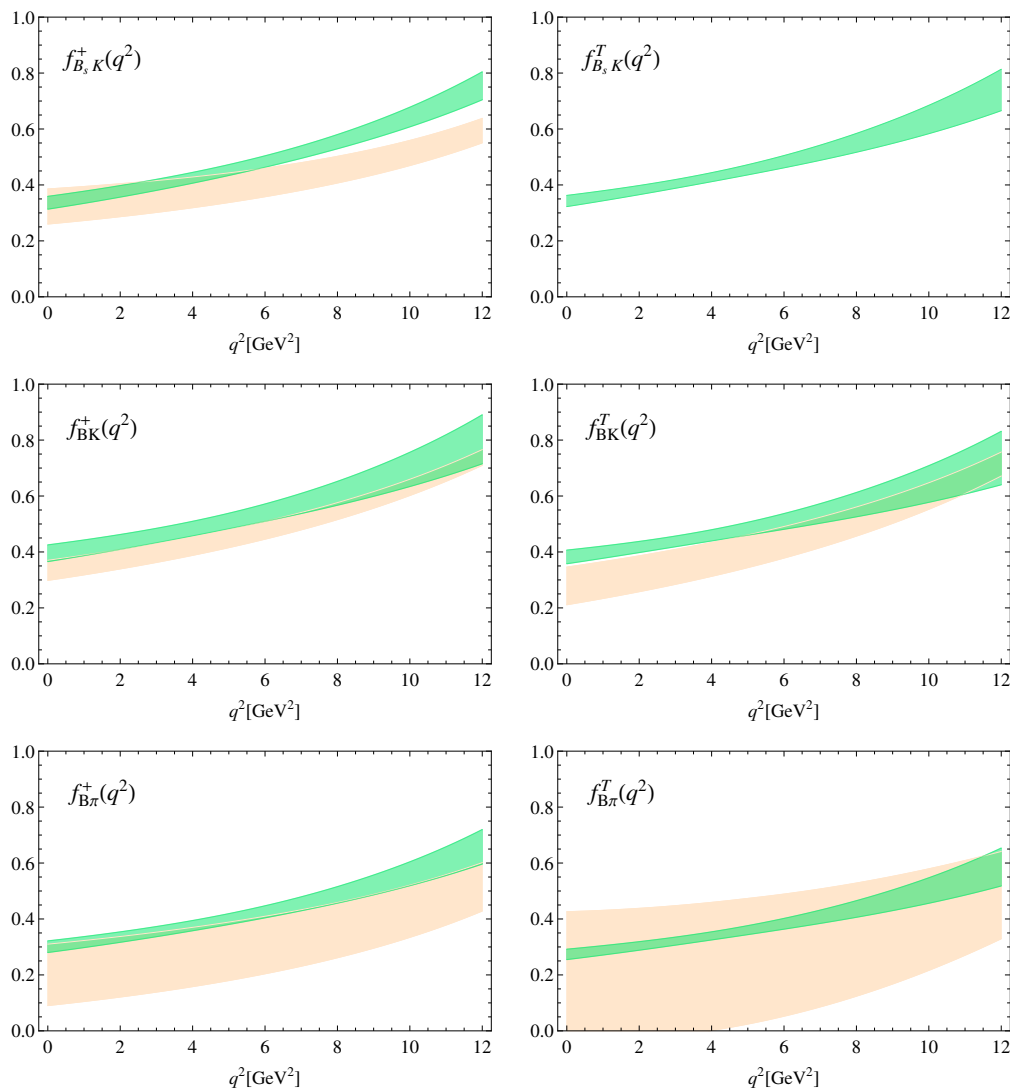


**Figure 1.** The vector (tensor) form factors of  $B_s \rightarrow K$ ,  $B \rightarrow K$  and  $B \rightarrow \pi$  transitions calculated from LCSRs including estimated parametrical uncertainties are shown on the upper, middle and lower left (right) panels, respectively, with the dark-shaded (green) bands. Extrapolations of the lattice QCD results for  $B_s \rightarrow K$  [23],  $B \rightarrow K$  [25] and  $B \rightarrow \pi$  [27, 28] form factors are shown with the light-shaded (orange) bands.

interval of our prediction, compared to the interval  $f_{B\pi}^+(0) = 0.26_{-0.03}^{+0.04}$  obtained in ref. [7]. The central value of the latter is somewhat below the one we present in table 2, since we use a smaller (larger) central input value of  $f_B$  (of  $\mu_\pi$ ). In ref. [7] one can also find a detailed comparison with the LCSR  $B \rightarrow \pi$  form factor obtained earlier in ref. [29].

We turn to the numerical analysis of  $B \rightarrow P\ell^+\ell^-$  observables, where the  $B \rightarrow P$  form factors obtained above are used. We recalculate the nonlocal amplitudes, following [12, 13]. In appendix B a brief outline of the calculational method is given. Here we need some additional input parameters. The most important are: the inverse moment  $\lambda_B$  of the  $B$ -meson DA (we assume  $\lambda_{B_s} = \lambda_B$ ) and the Borel and threshold parameters in  $\pi, K$  channel

Coefficient	$\mu = 2.5 \text{ GeV}$	$\mu = 3.0 \text{ GeV}$	$\mu = 4.5 \text{ GeV}$
$C_7^{\text{eff}}$	-0.332 (-0.356)	-0.321 (-0.343)	-0.304 (-0.316)
$C_9$	4.070 (4.514)	4.076 (4.462)	4.115 (4.293)
$C_{10}$	-4.122 (-4.493)	-4.122 (-4.493)	-4.122 (-4.493)

**Table 3.** Wilson coefficients of the FCNC operators at next-to-leading (leading) order in  $\alpha_s$  used in our numerical analysis at various scales.

Decay mode	$\mathcal{F}_{BP}[1.0, 6.0]$	$\mathcal{D}_{BP}[1.0, 6.0]$	$\mathcal{C}_{BP}[1.0, 6.0]$	$\mathcal{S}_{BP}[1.0, 6.0]$
$B^- \rightarrow K^- \ell^+ \ell^-$	$75.0^{+10.5}_{-9.7}$	—	—	—
$B^- \rightarrow \pi^- \ell^+ \ell^-$	$47.7^{+6.4}_{-5.9}$	$16.1^{+2.8}_{-10.1}$	$14.3^{+7.8}_{-5.8}$	$-9.8^{+7.1}_{-7.2}$
$\bar{B}_s \rightarrow K^0 \ell^+ \ell^-$	$61.0^{+7.0}_{-6.8}$	$7.8^{+3.4}_{-2.5}$	$-12.9^{+2.4}_{-2.2}$	$-3.4^{+1.1}_{-2.6}$

**Table 4.** The parts of the  $B \rightarrow P \ell^+ \ell^-$  amplitudes squared, as defined in eqs. (2.11)–(2.14), in the units  $[\text{GeV}^3]$ , for the bin  $[1.0 \text{ GeV}^2, 6.0 \text{ GeV}^2]$ .

in the LCSRs for the soft-gluon emission contributions. They are displayed in table 1. The same input parameters for the pion, kaon and  $B$ -meson DAs as the ones given in table 1 serve as an input in the hard-gluon contributions for which we use the QCD factorization expressions [14] at spacelike  $q^2$ .

The effective FCNC Hamiltonian (see eq. (B.1) in appendix B) is chosen as in [13] (see table V there), with all Wilson coefficients  $C_i$  taken at leading order in  $\alpha_s$ . This accuracy is sufficient for  $C_{1-6}, C_8^{\text{eff}}$  entering the nonlocal hadronic amplitudes, having in mind the overall accuracy of our method for these amplitudes. At the same time, the numerically large Wilson coefficients  $C_9, C_{10}$  and  $C_7^{\text{eff}}$  of the FCNC operators multiplying the factorizable parts of the decay amplitudes, have a noticeable impact on the observables. Therefore, we adopt here the values of these coefficients at the next-to-leading order in  $\alpha_s$  (see table 3).

For completeness and future use, in appendix B the numerical results for the separate nonlocal amplitudes  $\mathcal{H}_{BP}^{(u)}$  and  $\mathcal{H}_{BP}^{(c)}$  defined as in eq. (B.2) are presented in figures 2, 3, 4. Combining these results with the form factors, we compute the quantities defined in eq. (2.9) for a single bin  $[q_1^2, q_2^2] = [1.0 \text{ GeV}^2, 6.0 \text{ GeV}^2]$  which optimally covers the part of the large-recoil region. The results are collected in table 4, where the (uncorrelated) uncertainties are obtained by adding in quadrature the individual variations due to changes of input parameters.

Note that the binned quantities  $\mathcal{F}_{BP}$  are not much sensitive to the magnitude of the nonlocal amplitudes  $\mathcal{H}_{BP}^{(c)}(q^2)$ , which enter the numerically subleading contributions to the coefficients  $c_{BP}(q^2)$ . Hence, the differences between  $\mathcal{F}_{BK}, \mathcal{F}_{B\pi}$  and  $\mathcal{F}_{B_s K}$  in table 4 roughly

Decay mode	$B^- \rightarrow K^- \ell^+ \ell^-$	$B^- \rightarrow \pi^- \ell^+ \ell^-$	$\bar{B}_s \rightarrow K^0 \ell^+ \ell^-$
Measurement or calculation	$\mathcal{B}_{BK}[1.0, 6.0]$	$\mathcal{B}_{B\pi}[1.0, 6.0]$	$\mathcal{B}_{B_s K}[1.0, 6.0]$
Belle [31]	$2.72^{+0.46}_{-0.42} \pm 0.16$	—	—
CDF [32]	$2.58 \pm 0.36 \pm 0.16$	—	—
BaBar [33]	$2.72^{+0.54}_{-0.48} \pm 0.06$	—	—
LHCb [10, 34]	$2.42 \pm 0.7 \pm 0.12$	$0.091^{+0.021}_{-0.020} \pm 0.003$	—
HPQCD [38]	$3.62 \pm 1.22$	—	—
Fermilab/MILC [28, 39]	$3.49 \pm 0.62$	$0.096 \pm 0.013$	—
This work	$4.38^{+0.62}_{-0.57} \pm 0.28$	$0.131^{+0.023}_{-0.022} \pm 0.010$	$0.154^{+0.018}_{-0.017} \pm 0.011$

**Table 5.** Binned branching fractions in the units of  $10^{-8} \text{ GeV}^{-2}$  defined in eq. (2.15) for the bin  $[q_1^2, q_2^2] = [1.0 \text{ GeV}^2 - 6.0 \text{ GeV}^2]$ . The first (second) error in our predictions is due to the uncertainty of the input (only of the CKM parameters).

reflect the ratios of the corresponding form factors. On the other hand, the remaining binned quantities  $\mathcal{D}_{BP}$ ,  $\mathcal{C}_{BP}$  and  $\mathcal{S}_{BP}$  are essentially determined by the nonlocal effects in  $B \rightarrow P \ell^+ \ell^-$ . In particular, the large differences between  $\mathcal{D}_{B\pi}$ ,  $\mathcal{C}_{B\pi}$ ,  $\mathcal{S}_{B\pi}$  and  $\mathcal{D}_{B_s K}$ ,  $\mathcal{C}_{B_s K}$ ,  $\mathcal{S}_{B_s K}$  emerge mainly due to the enhancement of the weak annihilation mechanism in the nonlocal amplitude  $\mathcal{H}_{B\pi}^{(u)}(q^2)$  for  $B^- \rightarrow \pi^- \ell^+ \ell^-$  [13]. The same mechanism does not play a role in the amplitude  $\mathcal{H}_{B_s K}^{(u)}(q^2)$  contributing to  $\bar{B}_s \rightarrow K^0 \ell^+ \ell^-$ , due to a different quark content of the initial  $B_s$  meson, and due to a suppressed combination of Wilson coefficients.

As shown in the previous section, the binned quantities  $\mathcal{F}_{BP}$ ,  $\mathcal{D}_{BP}$ ,  $\mathcal{C}_{BP}$ ,  $\mathcal{S}_{BP}$  can in principle be used for an independent determination of the Wolfenstein parameters  $A$ ,  $\eta$  and  $\rho$  from the combination of observables measured in  $B \rightarrow P \ell^+ \ell^-$  decays. The important role in this determination is played by the direct  $CP$ -asymmetry in  $B \rightarrow \pi \ell^+ \ell^-$  which is not available yet in the large-recoil region bins. Hence, here we limit ourselves by an inverse procedure. Taking the values of all Wolfenstein parameters

$$\begin{aligned}
 \lambda &= 0.22506 \pm 0.00050, & A &= 0.811 \pm 0.026, \\
 \bar{\rho} = \rho \left(1 - \frac{\lambda^2}{2}\right) &= 0.124^{+0.019}_{-0.018}, & \bar{\eta} = \eta \left(1 - \frac{\lambda^2}{2}\right) &= 0.356 \pm 0.011, \quad (3.6)
 \end{aligned}$$

from the global fit of CKM matrix [17] and using the calculated hadronic input from table 4, we predict the values of the binned branching fractions presented in table 5 and the binned direct  $CP$ -asymmetries:

$$\mathcal{A}_{B\pi}[1.0, 6.0] = -0.15^{+0.11}_{-0.11}, \quad \mathcal{A}_{B_s K}[1.0, 6.0] = -0.04^{+0.01}_{-0.03}. \quad (3.7)$$

The numerical results for the  $B \rightarrow K \ell^+ \ell^-$  and  $B \rightarrow \pi \ell^+ \ell^-$  decays presented here update the previous ones obtained, respectively, in [12]<sup>4</sup> and [13].

<sup>4</sup>Note that the branching fractions given in the literature are adjusted to our definition, which implies division by the width  $(q_2^2 - q_1^2)$  of the bin.

## 4 Discussion

In this paper we updated the LCSR predictions for the  $B_s \rightarrow K$  form factors in the large recoil region of the kaon. We predicted the ratio of the integrated  $B_s \rightarrow K\ell\nu_\ell$  decay width and  $|V_{ub}|^2$ . Our result can be used to determine this CKM matrix element from the future data on  $B_s \rightarrow K\ell\nu_\ell$  in the kinematically dominant large recoil region.

We also calculated the hadronic input for the branching fractions and direct  $CP$ -asymmetries of  $B \rightarrow P\ell^+\ell^-$  FCNC decays in the large recoil bin  $1.0 \leq q^2 \leq 6.0 \text{ GeV}^2$ . Our results include the  $B \rightarrow P$  form factors and nonlocal hadronic matrix elements, all obtained in the same framework and with a uniform input. The LCSRs used in this calculation take into account the soft-overlap nonfactorizable contributions to the form factors and nonlocal amplitudes. Extending the application of LCSRs to other nonlocal contributions represents an important task for the future. For example, as discussed in more detail in [13], the weak annihilation contribution which is important in the  $B \rightarrow \pi\ell^+\ell^-$  decay can be obtained from LCSRs with  $B$ -meson DAs, alternative to QCD factorization and potentially including subleading effects.

Furthermore, we suggested a systematic way to extract the CKM matrix elements, cast in a form of the Wolfenstein parameters, from the combination of observables in  $B \rightarrow P\ell^+\ell^-$  decays, independent of the other methods involving the nonleptonic  $B$ -decays and/or  $B - \bar{B}$  mixing.

Note that an independent extraction of CKM parameters is also possible from other modes of FCNC exclusive  $B$ -decays, such as  $B_{(s)} \rightarrow V\gamma$  or  $B_{(s)} \rightarrow V\ell^+\ell^-$ , where  $V = K^*, \rho$ . The corresponding combinations of observables demand, apart from  $B \rightarrow V$  form factors, a dedicated calculation of all relevant nonlocal hadronic matrix elements. For this not yet accomplished task, a variety of methods combining QCD factorization with various versions of LCSRs may prove to be useful. In case of radiative decays the sum rules with photon and vector-meson DAs and heavy-meson interpolating currents can be also of use (for previous works in this direction see [35–37]).

In table 5 we compare our results for the binned branching fractions<sup>4</sup> with the experimental measurements and lattice QCD predictions [28, 38, 39]. In the lattice QCD studies of  $B \rightarrow P\ell^+\ell^-$  decays, as explained in detail in [39], the nonlocal contributions cannot be calculated in a fully model-independent way. Instead, the (continuum) QCD-factorization [14] in the timelike region of  $q^2$  is employed. Let us also mention in this context the earlier estimates of  $B \rightarrow K\ell\ell$  [40, 41] and  $B \rightarrow \pi\ell\ell$  [42] where the QCD-factorization approach was used combined with various inputs and extrapolations for the form factors.

As seen from table 5, the theory predictions for the  $B \rightarrow K\ell^+\ell^-$  branching fraction reveal some tension with the experimentally measured values, making this observable an important ingredient of the global fits of rare  $B$  decays (see e.g., [43]). Adding the characteristics of  $B \rightarrow \pi\ell^+\ell^-$  and  $B_s \rightarrow K\ell^+\ell^-$  decays to the set of fitted observables will further extend the possibilities to test the Standard Model in the quark-flavour sector. The fact that these very rare  $B$ -decay modes are within the reach of LHCb experiment, makes this task realistic.

## Acknowledgments

We thank Danny van Dyk and Yu-Ming Wang for useful discussions. This work is supported by the DFG Research Unit FOR 1873 “Quark Flavour Physics and Effective Theories”, contract No KH 205/2-2. AK is grateful for support to the Munich Institute for Astro- and Particle Physics (MIAPP) of the DFG cluster of excellence “Origin and Structure of the Universe” where the part of this work was done. AR acknowledges the Nikolai-Uraltsev Fellowship of Siegen University and the partial support of the Russian Foundation for Basic Research (project No. 15-02-06033-a).

## A LCSR calculation of the $B \rightarrow P$ form factors

The LCSRs for  $B \rightarrow P$  ( $P = \pi, K$ ) form factors at large recoil of  $P$  (parametrically, at  $q^2 \ll m_b^2$ ) are derived from the correlation function of the weak flavour-changing current and  $B$ -interpolating quark current, sandwiched between the vacuum and on-shell  $P$ -state:

$$\begin{aligned}
 F_{BP}^\mu(p, q) &= i \int d^4x e^{iqx} \langle P(p) | T \{ \bar{q}_1(x) \Gamma^\mu b(x), (m_b + m_{q_2}) \bar{b}(0) i \gamma_5 q_2(0) \} | 0 \rangle \\
 &= \begin{cases} F_{BP}(q^2, (p+q)^2) p^\mu + \tilde{F}_{BP}(q^2, (p+q)^2) q^\mu, & \Gamma^\mu = \gamma^\mu, \\ F_{BP}^T(q^2, (p+q)^2) [q^2 p^\mu - (q \cdot p) q^\mu], & \Gamma^\mu = -i \sigma^{\mu\nu} q_\nu, \end{cases} \quad (\text{A.1})
 \end{aligned}$$

where the quark-flavour combination  $q_1 = u, q_2 = s$  corresponds to the  $\bar{B}_s \rightarrow K^+$  weak transition;  $q_1 = s, q_2 = u$  and  $q_1 = d$  and  $q_2 = u$  ( $q_2 = s$ ) correspond, respectively to the  $B^- \rightarrow K^-$  and  $B^- \rightarrow \pi^-$  ( $\bar{B}_s \rightarrow K^0$ ) FCNC transitions.

The invariant amplitudes  $F_{BP}(q^2, (p+q)^2)$  and  $F_{BP}^T(q^2, (p+q)^2)$  in (A.1) are used to derive the LCSRs for the vector  $f_{BP}^+(q^2)$  and tensor  $f_{BP}^T(q^2)$  form factors, respectively. At  $q^2 \ll m_b^2$  and  $(p+q)^2 \ll m_b^2$  the OPE near the light-cone  $x^2 \simeq 0$  is applied for the correlation function (A.1) and the result is cast in a form of convolution, e.g.:

$$F_{BP}^{(\text{OPE})}(q^2, (p+q)^2) = \sum_{t=2,3,4,\dots} \int \mathcal{D}u \sum_{k=0,1,\dots} \left( \frac{\alpha_s(\mu)}{\pi} \right)^k T_k^{(t)}(q^2, (p+q)^2, \{u_i\}) \varphi_P^{(t)}(\{u_i\}, \mu), \quad (\text{A.2})$$

where  $T_k^{(t)}$  are the perturbatively calculable hard-scattering amplitudes and  $\varphi_P^{(t)}(u_i)$  are the  $P$ -meson light-cone distribution amplitudes (DAs) of the twist  $t \geq 2$ . The variables  $\{u_i\} = \{u_1, u_2, \dots\}$  are the fractions of the  $P$ -meson momentum carried by the constituents of DAs and  $\mathcal{D}u = \delta(1 - \sum_i u_i) \prod_i du_i$ . In eq. (A.2) the same renormalization scale  $\mu$  is used for DAs and for the QCD running parameters in the adopted  $\overline{MS}$  scheme.

The terms in the eq. (A.2) that correspond to higher-twist light meson DAs are suppressed by inverse powers of the  $b$ -quark virtuality  $\sim ((p+q)^2 - m_b^2) \sim \bar{\Lambda} m_b$ , where  $\bar{\Lambda} \gg \Lambda_{\text{QCD}}$  does not scale with  $m_b$ . The adopted approximation for the correlation function includes LO contributions of the twist 2,3,4 quark-antiquark and quark-antiquark-gluon DAs. For the kaon DAs the  $O(m_K^2) \sim O(m_s)$  accuracy is adopted. The factorizable parts of twist-5,6 contributions to LCSRs for  $B \rightarrow P$  form factors were calculated by one of us [9] and their numerical impact on the total invariant amplitude was found negligible,

$< 0.1\%$  of the total. This strengthens the argument for using a truncated twist expansion to the accuracy  $t = 4$ .

The NLO  $O(\alpha_s)$  corrections to the twist-2 and (two-particle) twist-3 hard-scattering amplitudes  $T_1^{(2,3)}$  are taken into account. In the latter we neglect the  $s$ -quark mass, hence, the double suppressed  $O(\alpha_s m_s/\bar{\Lambda})$  effects. We use the expressions for OPE derived in [7] extending them to the  $B \rightarrow K$  and  $B_s \rightarrow K$  cases (see also [18]). We do not include the  $O(\beta_0)$  estimate of the twist-2  $O(\alpha_s^2)$  contribution to the twist-2 hard-scattering amplitude calculated in [44], since the resulting effect in LSCR is very small and does not yet represent a complete NNLO computation of  $T_1^{(2)}$ .

The analytic result for  $F_{BP}^{(\text{OPE})}(q^2, (p+q)^2)$  and  $F_{BP}^{T(\text{OPE})}(q^2, (p+q)^2)$  is matched to the hadronic dispersion relation for the correlation function (A.1) in the variable  $(p+q)^2$ . To apply quark-hadron duality one needs to transform the calculated invariant amplitudes to the form of dispersion integral,

$$F_{BP}^{(T)(\text{OPE})}(q^2, (p+q)^2) = \frac{1}{\pi} \int_{m_b^2}^{\infty} ds \frac{\text{Im}F_{BP}^{(T)(\text{OPE})}(q^2, s)}{s - (p+q)^2}. \quad (\text{A.3})$$

We equate the contribution of the excited and continuum  $B$ -states in the hadronic dispersion relation to the part of the above integral at  $s > s_0^B$ , where  $s_0^B$  is the effective, process-dependent threshold. The integral at  $s \leq s_0^B$  is then equated to the contribution of the ground-state of  $B$ -meson. The subsequent Borel transformation with respect to the variable  $(p+q)^2$  exponentiates denominators, so that, e.g.,  $1/[s - (p+q)^2] \rightarrow e^{-s/M^2}$ . Here  $M^2$  is the Borel parameter chosen so that  $M^2 \sim \bar{\Lambda} m_b \sim \mu^2$  guarantees a power suppression of higher-twist contributions. One finally obtains the LCSRs for the  $B \rightarrow P$  form factors:

$$f_{BP}^+(q^2) = \frac{e^{m_B^2/M^2}}{2m_B^2 f_B} \frac{1}{\pi} \int_{m_b^2}^{s_0^B} ds \text{Im}F_{BP}^{(\text{OPE})}(q^2, s) e^{-s/M^2},$$

$$f_{BP}^T(q^2) = \frac{(m_B + m_P) e^{m_B^2/M^2}}{2m_B^2 f_B} \frac{1}{\pi} \int_{m_b^2}^{s_0^B} ds \text{Im}F_{BP}^{T(\text{OPE})}(q^2, s) e^{-s/M^2}. \quad (\text{A.4})$$

## B Nonlocal contributions to $B \rightarrow P\ell^+\ell^-$

The effective weak Hamiltonian of the  $b \rightarrow q\ell^+\ell^-$  transitions ( $q = d, s$ ) generating the  $B \rightarrow P\ell^+\ell^-$  decays has the following form in the Standard Model (see e.g., the review [45]):

$$H_{\text{eff}}^{b \rightarrow q} = \frac{4G_F}{\sqrt{2}} \left( \lambda_u^{(q)} \sum_{i=1}^2 C_i \mathcal{O}_i^u + \lambda_c^{(q)} \sum_{i=1}^2 C_i \mathcal{O}_i^c - \lambda_t^{(q)} \sum_{i=3}^{10} C_i \mathcal{O}_i \right) + h.c., \quad (\text{B.1})$$

where  $\lambda_p^{(q)} = V_{pb} V_{pq}^*$ , ( $p = u, c, t$ ) are the products of CKM matrix elements. For the  $B \rightarrow K\ell^+\ell^-$  transitions, the part of the decay amplitude proportional to  $\lambda_u^{(s)} \sim \lambda^4$  is neglected. The operators  $\mathcal{O}_i$  in (B.1) and the numerical values of their Wilson coefficients  $C_i$



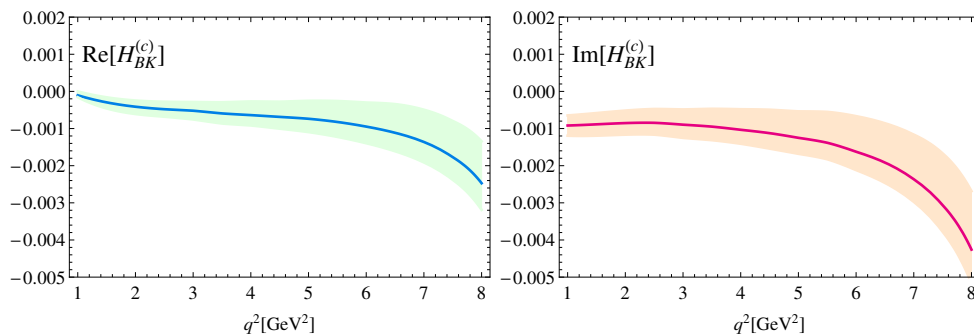


**Figure 2.** Hadronic nonlocal amplitude  $\mathcal{H}_{BK}^{(c)}(q^2)$  in  $B^- \rightarrow K^- \ell^+ \ell^-$  in the large recoil region. On the left (right) panel the real (imaginary) part is plotted for the central input (solid) and including uncertainties (dashed band).

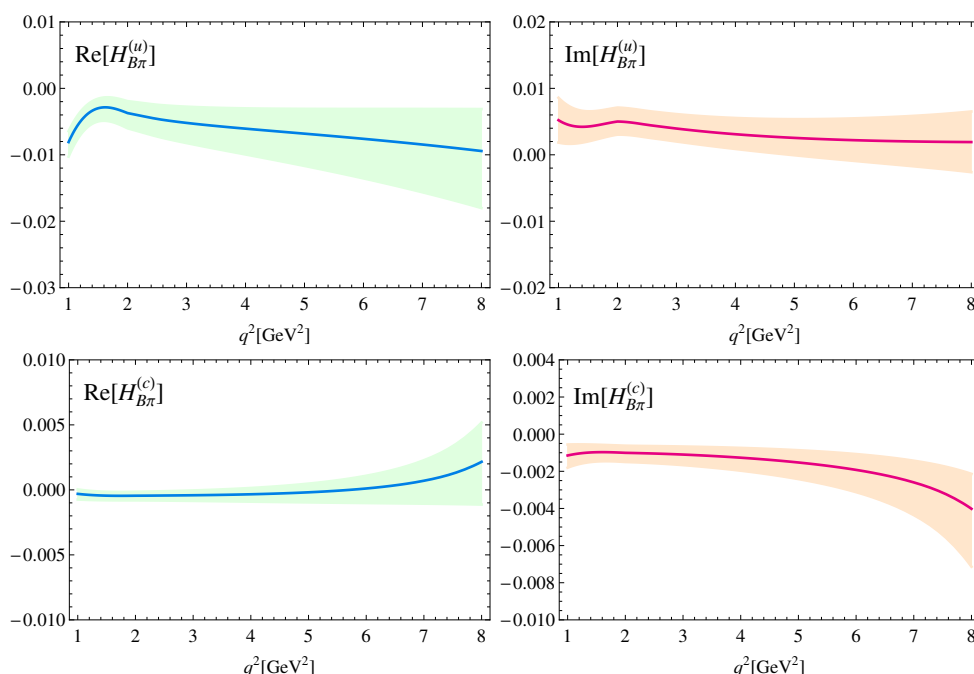


**Figure 3.** The same as in figure 2 for the amplitudes  $\mathcal{H}_{B\pi}^{(u)}(q^2)$  and  $\mathcal{H}_{B\pi}^{(c)}(q^2)$  in  $B^- \rightarrow \pi^- \ell^+ \ell^-$ .

used in this paper are listed in the appendix A of ref. [13] and in table 3 above. In the decay amplitude (2.4) the dominant contributions of the operators  $\mathcal{O}_{9,10}$  and  $\mathcal{O}_7$  are factorized to the  $B \rightarrow P$  form factors. The additional amplitudes denoted as  $\mathcal{H}_{BP}^{(c)}(q^2)$ ,  $\mathcal{H}_{BP}^{(u)}(q^2)$  in eqs. (2.5), (2.6) accumulate the nonlocal effects generated by the all remaining effective operators combined with the electromagnetic emission of the lepton pair. They can be represented as a correlation function of the time-ordered product of effective operators with

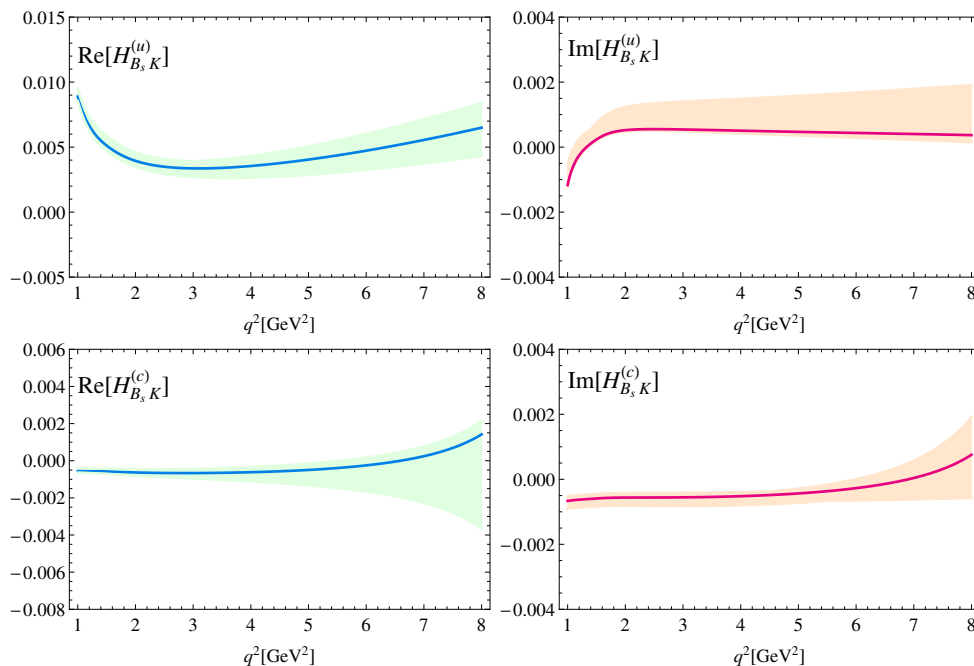


**Figure 4.** The same as in figure 2 for the amplitudes  $\mathcal{H}_{B_s K}^{(u)}(q^2)$  and  $\mathcal{H}_{B_s K}^{(c)}(q^2)$  in  $\bar{B}_s \rightarrow K^0 \ell^+ \ell^-$ .

the quark e.m. current,  $j_\mu^{\text{em}} = \sum_{q=u,d,s,c,b} Q_q \bar{q} \gamma_\mu q$ , sandwiched between  $B$  and  $P$  states:

$$\begin{aligned} \mathcal{H}_{(BP)\mu}^{(p)} &= i \int d^4 x e^{iqx} \langle P(p) | \text{T} \left\{ j_\mu^{\text{em}}(x), \left[ C_1 \mathcal{O}_1^p(0) + C_2 \mathcal{O}_2^p(0) + \sum_{k=3-6,8g} C_k \mathcal{O}_k(0) \right] \right\} | B(p+q) \rangle \\ &= [(p \cdot q) q_\mu - q^2 p_\mu] \mathcal{H}_{BP}^{(p)}(q^2), \quad (p = u, c). \end{aligned} \quad (\text{B.2})$$

In the case of the  $B \rightarrow K \ell^+ \ell^-$  decay only the amplitude  $\mathcal{H}_{BK}^{(c)}(q^2)$  contributes. The calculation of the nonlocal amplitudes following the method suggested in [11] proceeds in two stages. First, the amplitudes  $\mathcal{H}_{BP}^{(c,u)}(q^2)$  are splitted in the contributions with different topologies, including  $c$  or  $u$  quark emission in LO, NLO factorizable corrections, nonfactorizable effects of soft gluon emission, hard-spectator and annihilation contributions. They are calculated one by one at spacelike  $q^2 < 0$  where the light-cone OPE for the correlation function (B.2) is valid. For the hard-gluon NLO and spectator contributions we apply the QCD factorization and for the soft gluon emission the dedicated LCSRs. A detailed account of this calculation can be found in refs. [12] and [13]. After that, the resulting functions  $\mathcal{H}_{BP}^{(c,u)}(q^2 < 0)$  are fitted to the hadronic dispersion relations in the  $q^2$  variable where the contributions from the lowest vector mesons  $V = \rho, \omega, \phi, J/\psi, \psi(2S)$  are isolated and the excited states and continuum contributions are modeled, employing the quark-hadron duality. Here we employ as an additional input the experimental data on branching fractions of the nonleptonic  $B \rightarrow VP$  decays determining together with the vector meson decay constants the moduli of the residues in the pole terms of the dispersion relation. The phases of these contributions are included in the set of fit parameters. Since in this paper we are interested only in the large recoil (low  $q^2$ ) region, the integral over

hadronic spectral density at  $q^2 > 4m_D^2$  with no singularities in the large recoil region is modeled by a polynomial with complex parameters (see refs. [12, 13] for details). Indeed, for our purposes it is not necessary to use a more detailed hadronic representation, like the ansatz suggested in [46] and used in [47], where the broad charmonium resonances located above the open charm threshold are resolved with separate relative phases.

Having fitted the parameters of dispersion relations, we continue them to the positive values of  $q^2$  in the large recoil region, where there is a minor influence of the model-dependent contributions. Finally, we note that in our approach the differences between the  $B_s \rightarrow K$ ,  $B \rightarrow K$  and  $B \rightarrow \pi$  nonlocal amplitudes originate from the  $SU(3)_{fl}$ -violating differences between the decay constants, parameters of light-meson DAs and nonleptonic amplitudes, as well as from the different spectator-quark flavours, determining the diagram content of these amplitudes.

**Open Access.** This article is distributed under the terms of the Creative Commons Attribution License ([CC-BY 4.0](https://creativecommons.org/licenses/by/4.0/)), which permits any use, distribution and reproduction in any medium, provided the original author(s) and source are credited.

## References

- [1] T. Mannel and R. Kowalewski, *Semileptonic bottom hadron decays and the determination of  $V_{cb}$  and  $V_{ub}$* , in PARTICLE DATA GROUP collaboration, C. Patrignani et al., *Review of Particle Physics*, *Chin. Phys. C* **40** (2016) 100001 [[INSPIRE](#)].
- [2] T. Feldmann, B. Müller and D. van Dyk, *Analyzing  $b \rightarrow u$  transitions in semileptonic  $\bar{B}_s \rightarrow K^{*+}(\rightarrow K\pi)\ell^- \bar{\nu}_\ell$  decays*, *Phys. Rev. D* **92** (2015) 034013 [[arXiv:1503.09063](#)] [[INSPIRE](#)].
- [3] I.I. Balitsky, V.M. Braun and A.V. Kolesnichenko,  $\Sigma^+ \rightarrow P\gamma$  Decay in QCD (in Russian), *Sov. J. Nucl. Phys.* **44** (1986) 1028 [*Yad. Fiz.* **44** (1986) 1582] [[INSPIRE](#)].
- [4] I.I. Balitsky, V.M. Braun and A.V. Kolesnichenko, *Radiative Decay  $\Sigma^+ \rightarrow p\gamma$  in Quantum Chromodynamics*, *Nucl. Phys. B* **312** (1989) 509 [[INSPIRE](#)].
- [5] V.L. Chernyak and I.R. Zhitnitsky, *B meson exclusive decays into baryons*, *Nucl. Phys. B* **345** (1990) 137 [[INSPIRE](#)].
- [6] G. Duplancic and B. Melic,  *$B, B(s) \rightarrow K$  form factors: An update of light-cone sum rule results*, *Phys. Rev. D* **78** (2008) 054015 [[arXiv:0805.4170](#)] [[INSPIRE](#)].
- [7] G. Duplancic, A. Khodjamirian, T. Mannel, B. Melic and N. Offen, *Light-cone sum rules for  $B \rightarrow \pi$  form factors revisited*, *JHEP* **04** (2008) 014 [[arXiv:0801.1796](#)] [[INSPIRE](#)].
- [8] P. Gelhausen, A. Khodjamirian, A.A. Pivovarov and D. Rosenthal, *Decay constants of heavy-light vector mesons from QCD sum rules*, *Phys. Rev. D* **88** (2013) 014015 [*Erratum ibid.* **89** (2014) 099901] [*Erratum ibid.* **91** (2015) 099901] [[arXiv:1305.5432](#)] [[INSPIRE](#)].
- [9] A.V. Rusov, *Higher-twist effects in light-cone sum rule for the  $B \rightarrow \pi$  form factor*, *Eur. Phys. J. C* **77** (2017) 442 [[arXiv:1705.01929](#)] [[INSPIRE](#)].
- [10] LHCb collaboration, *First measurement of the differential branching fraction and CP asymmetry of the  $B^\pm \rightarrow \pi^\pm \mu^+ \mu^-$  decay*, *JHEP* **10** (2015) 034 [[arXiv:1509.00414](#)] [[INSPIRE](#)].

- [11] A. Khodjamirian, T. Mannel, A.A. Pivovarov and Y.M. Wang, *Charm-loop effect in  $B \rightarrow K^{(*)}\ell^+\ell^-$  and  $B \rightarrow K^*\gamma$* , *JHEP* **09** (2010) 089 [[arXiv:1006.4945](#)] [[INSPIRE](#)].
- [12] A. Khodjamirian, T. Mannel and Y.M. Wang,  *$B \rightarrow K\ell^+\ell^-$  decay at large hadronic recoil*, *JHEP* **02** (2013) 010 [[arXiv:1211.0234](#)] [[INSPIRE](#)].
- [13] C. Hambrock, A. Khodjamirian and A. Rusov, *Hadronic effects and observables in  $B \rightarrow \pi\ell^+\ell^-$  decay at large recoil*, *Phys. Rev.* **D 92** (2015) 074020 [[arXiv:1506.07760](#)] [[INSPIRE](#)].
- [14] M. Beneke, T. Feldmann and D. Seidel, *Systematic approach to exclusive  $B \rightarrow V\ell^+\ell^-$ ,  $V\gamma$  decays*, *Nucl. Phys.* **B 612** (2001) 25 [[hep-ph/0106067](#)] [[INSPIRE](#)].
- [15] A. Khodjamirian, T. Mannel, N. Offen and Y.M. Wang,  *$B \rightarrow \pi\ell\nu_\ell$  Width and  $|V_{ub}|$  from QCD Light-Cone Sum Rules*, *Phys. Rev.* **D 83** (2011) 094031 [[arXiv:1103.2655](#)] [[INSPIRE](#)].
- [16] I. Sentitemsu Imsong, A. Khodjamirian, T. Mannel and D. van Dyk, *Extrapolation and unitarity bounds for the  $B \rightarrow \pi$  form factor*, *JHEP* **02** (2015) 126 [[arXiv:1409.7816](#)] [[INSPIRE](#)].
- [17] PARTICLE DATA GROUP collaboration, C. Patrignani et al., *Review of Particle Physics*, *Chin. Phys.* **C 40** (2016) 100001 [[INSPIRE](#)] also <http://pdg.lbl.gov>.
- [18] A. Khodjamirian, C. Klein, T. Mannel and N. Offen, *Semileptonic charm decays  $D \rightarrow \pi\ell\nu_\ell$  and  $D \rightarrow K\ell\nu_\ell$  from QCD Light-Cone Sum Rules*, *Phys. Rev.* **D 80** (2009) 114005 [[arXiv:0907.2842](#)] [[INSPIRE](#)].
- [19] K.G. Chetyrkin, A. Khodjamirian and A.A. Pivovarov, *Towards NNLO Accuracy in the QCD Sum Rule for the Kaon Distribution Amplitude*, *Phys. Lett.* **B 661** (2008) 250 [[arXiv:0712.2999](#)] [[INSPIRE](#)].
- [20] H. Leutwyler, *The ratios of the light quark masses*, *Phys. Lett.* **B 378** (1996) 313 [[hep-ph/9602366](#)] [[INSPIRE](#)].
- [21] P. Ball, V.M. Braun and A. Lenz, *Higher-twist distribution amplitudes of the  $K$  meson in QCD*, *JHEP* **05** (2006) 004 [[hep-ph/0603063](#)] [[INSPIRE](#)].
- [22] C. Bourrely, I. Caprini and L. Lellouch, *Model-independent description of  $B \rightarrow \pi\ell\nu$  decays and a determination of  $|V_{ub}|$* , *Phys. Rev.* **D 79** (2009) 013008 [*Erratum ibid.* **D 82** (2010) 099902] [[arXiv:0807.2722](#)] [[INSPIRE](#)].
- [23] C.M. Bouchard, G.P. Lepage, C. Monahan, H. Na and J. Shigemitsu,  *$B_s \rightarrow K\ell\nu$  form factors from lattice QCD*, *Phys. Rev.* **D 90** (2014) 054506 [[arXiv:1406.2279](#)] [[INSPIRE](#)].
- [24] ALPHA collaboration, F. Bahr et al., *Continuum limit of the leading-order HQET form factor in  $B_s \rightarrow K\ell\nu$  decays*, *Phys. Lett.* **B 757** (2016) 473 [[arXiv:1601.04277](#)] [[INSPIRE](#)].
- [25] J.A. Bailey et al.,  *$B \rightarrow K\ell^+\ell^-$  decay form factors from three-flavor lattice QCD*, *Phys. Rev.* **D 93** (2016) 025026 [[arXiv:1509.06235](#)] [[INSPIRE](#)].
- [26] HPQCD collaboration, C. Bouchard, G.P. Lepage, C. Monahan, H. Na and J. Shigemitsu, *Rare decay  $B \rightarrow K\ell^+\ell^-$  form factors from lattice QCD*, *Phys. Rev.* **D 88** (2013) 054509 [*Erratum ibid.* **D 88** (2013) 079901] [[arXiv:1306.2384](#)] [[INSPIRE](#)].
- [27] FERMILAB LATTICE and MILC collaborations, J.A. Bailey et al.,  *$|V_{ub}|$  from  $B \rightarrow \pi\ell\nu$  decays and  $(2+1)$ -flavor lattice QCD*, *Phys. Rev.* **D 92** (2015) 014024 [[arXiv:1503.07839](#)] [[INSPIRE](#)].
- [28] FERMILAB LATTICE and MILC collaborations, J.A. Bailey et al.,  *$B \rightarrow \pi\ell\ell$  form factors for new-physics searches from lattice QCD*, *Phys. Rev. Lett.* **115** (2015) 152002 [[arXiv:1507.01618](#)] [[INSPIRE](#)].

- [29] P. Ball and R. Zwicky, *New results on  $B \rightarrow \pi, K, \eta$  decay formfactors from light-cone sum rules*, *Phys. Rev. D* **71** (2005) 014015 [[hep-ph/0406232](#)] [[INSPIRE](#)].
- [30] V.M. Braun, D. Yu. Ivanov and G.P. Korchemsky, *The  $B$  meson distribution amplitude in QCD*, *Phys. Rev. D* **69** (2004) 034014 [[hep-ph/0309330](#)] [[INSPIRE](#)].
- [31] BELLE collaboration, J.T. Wei et al., *Measurement of the Differential Branching Fraction and Forward-Backward Asymmetry for  $B \rightarrow K^{(*)}\ell^+\ell^-$* , *Phys. Rev. Lett.* **103** (2009) 171801 [[arXiv:0904.0770](#)] [[INSPIRE](#)].
- [32] CDF collaboration, T. Aaltonen et al., *Observation of the Baryonic Flavor-Changing Neutral Current Decay  $\Lambda_b \rightarrow \Lambda\mu^+\mu^-$* , *Phys. Rev. Lett.* **107** (2011) 201802 [[arXiv:1107.3753](#)] [[INSPIRE](#)].
- [33] BABAR collaboration, J.P. Lees et al., *Measurement of Branching Fractions and Rate Asymmetries in the Rare Decays  $B \rightarrow K^{(*)}l^+l^-$* , *Phys. Rev. D* **86** (2012) 032012 [[arXiv:1204.3933](#)] [[INSPIRE](#)].
- [34] LHCb collaboration, *Differential branching fractions and isospin asymmetries of  $B \rightarrow K^{(*)}\mu^+\mu^-$  decays*, *JHEP* **06** (2014) 133 [[arXiv:1403.8044](#)] [[INSPIRE](#)].
- [35] A. Khodjamirian, G. Stoll and D. Wyler, *Calculation of long distance effects in exclusive weak radiative decays of  $B$  meson*, *Phys. Lett. B* **358** (1995) 129 [[hep-ph/9506242](#)] [[INSPIRE](#)].
- [36] A. Ali and V.M. Braun, *Estimates of the weak annihilation contributions to the decays  $B \rightarrow \rho + \gamma$  and  $B \rightarrow \omega + \gamma$* , *Phys. Lett. B* **359** (1995) 223 [[hep-ph/9506248](#)] [[INSPIRE](#)].
- [37] J. Lyon and R. Zwicky, *Isospin asymmetries in  $B \rightarrow (K^*, \rho)\gamma/l^+l^-$  and  $B \rightarrow Kl^+l^-$  in and beyond the standard model*, *Phys. Rev. D* **88** (2013) 094004 [[arXiv:1305.4797](#)] [[INSPIRE](#)].
- [38] HPQCD collaboration, C. Bouchard, G.P. Lepage, C. Monahan, H. Na and J. Shigemitsu, *Standard Model Predictions for  $B \rightarrow K\ell^+\ell^-$  with Form Factors from Lattice QCD*, *Phys. Rev. Lett.* **111** (2013) 162002 [[arXiv:1306.0434](#)] [[INSPIRE](#)].
- [39] D. Du et al., *Phenomenology of semileptonic  $B$ -meson decays with form factors from lattice QCD*, *Phys. Rev. D* **93** (2016) 034005 [[arXiv:1510.02349](#)] [[INSPIRE](#)].
- [40] C. Bobeth, G. Hiller and D. van Dyk, *General analysis of  $\bar{B} \rightarrow \bar{K}^{(*)}\ell^+\ell^-$  decays at low recoil*, *Phys. Rev. D* **87** (2013) 034016 [[arXiv:1212.2321](#)] [[INSPIRE](#)].
- [41] W. Altmannshofer and D.M. Straub, *Cornering New Physics in  $b \rightarrow s$  Transitions*, *JHEP* **08** (2012) 121 [[arXiv:1206.0273](#)] [[INSPIRE](#)].
- [42] A. Ali, A. Ya. Parkhomenko and A.V. Rusov, *Precise Calculation of the Dilepton Invariant-Mass Spectrum and the Decay Rate in  $B^\pm \rightarrow \pi^\pm\mu^+\mu^-$  in the SM*, *Phys. Rev. D* **89** (2014) 094021 [[arXiv:1312.2523](#)] [[INSPIRE](#)].
- [43] S. Descotes-Genon, L. Hofer, J. Matias and J. Virto, *Global analysis of  $b \rightarrow s\ell\ell$  anomalies*, *JHEP* **06** (2016) 092 [[arXiv:1510.04239](#)] [[INSPIRE](#)].
- [44] A. Bharucha, *Two-loop Corrections to the  $B\text{to}\pi$  Form Factor from QCD Sum Rules on the Light-Cone and  $|V_{ub}|$* , *JHEP* **05** (2012) 092 [[arXiv:1203.1359](#)] [[INSPIRE](#)].
- [45] G. Buchalla, A.J. Buras and M.E. Lautenbacher, *Weak decays beyond leading logarithms*, *Rev. Mod. Phys.* **68** (1996) 1125 [[hep-ph/9512380](#)] [[INSPIRE](#)].
- [46] J. Lyon and R. Zwicky, *Resonances gone topsy turvy - the charm of QCD or new physics in  $b \rightarrow s\ell^+\ell^-$ ?*, [[arXiv:1406.0566](#)] [[INSPIRE](#)].
- [47] LHCb collaboration, *Measurement of the phase difference between short- and long-distance amplitudes in the  $B^+ \rightarrow K^+\mu^+\mu^-$  decay*, *Eur. Phys. J. C* **77** (2017) 161 [[arXiv:1612.06764](#)] [[INSPIRE](#)].